Available online at www.sciencedirect.com
SCIENCE DIRECT®
Pergamon
Materials Research Bulletin 38 (2003) 1773–1779
Materials Research Bulletin
www.elsevier.com/locate/matresbu

Structural and vibrational studies of $NaZr_2(AsO_4)_3$

M. Chakir[a], A.El. Jazouli[a,*], D.de Waal[b]

[a]*Laboratoire de Chimie des Matériaux Solides, Faculté des Sciences Ben M'Sik, UH2M, Boulevard Idriss El Harti, B.P. 7955 Casablanca, Morocco*
[b]*Department of Chemistry, University of Pretoria, 0002 Pretoria, South Africa*

Received 31 May 2002; received in revised form 5 November 2002; accepted 29 January 2003

Abstract

The structure of $NaZr_2(AsO_4)_3$, which belongs to the Nasicon-type family, was solved by the Rietveld method in the $R\bar{3}c$ space group, from X-ray powder diffraction data. The hexagonal unit cell parameters are $a_h = 9.1518(2)$ Å and $c_h = 23.1097(4)$ Å. The structure is formed by a three-dimensional network of AsO_4 tetrahedra and ZrO_6 octahedra sharing corners. Na atoms occupy totally the M1 site. Raman and infrared spectra were recorded and assignments of the As–O stretching and bending modes were made.

Keywords: A. Inorganic compound; C. X-ray diffraction; C. Infrared spectroscopy; C. Raman spectroscopy

1. Introduction

Nasicon-type materials have been extensively studied in context of various fields of solid state chemistry: solid electrolytes, electrode materials, low thermal expansion ceramics, etc. [1–9]. Their structure was initially described for $NaA_2(PO_4)_3$ (A = Ti, Zr, Ge) [1]. It consists of a three-dimensional (3D) network built up of PO_4 tetrahedra sharing corners with AO_6 octahedra. Within the 3D-framework, two sites, usually labelled M1 and M2, are available for the alkali metal cations. The M1 site is an antiprism formed by the triangular faces of two AO_6 octahedra along *c*-axis of the hexagonal cell. Thus, the network of $NaA_2(PO_4)_3$ can be considered as made up of infinite ribbons of composition $(O_3AO_3M1(Na)O_3AO_3)_\infty$ connected by PO_4 tetrahedra. The M2 sites are located between these ribbons in large cavities with a eight-fold coordination. The M1 and M2 sites may be completely empty as in $NbTi(PO_4)_3$ [10], partially occupied as in $NaZr_2(PO_4)_3$ [1] and $Na_3CaTi(PO_4)_3$ [11], or fully occupied as in $Na_5Ti(PO_4)_3$ [12]. In contrast to the extensive studies of the Nasicon-type phosphates and silicates, only a few investigations have been reported for the arsenates analogues. To our knowledge only X-ray

* Corresponding author. Fax: +212-22-70-46.
E-mail address: a.eljazouli@univh2m.ac.ma (A.El. Jazouli).

0025-5408/$ – see front matter
doi:10.1016/S0025-5408(03)00104-1

Table 1
Crystallographic data for $NaZr_2(AsO_4)3$

Wavelength (Å)	$\lambda_{K\alpha1} = 1.5406$; $\lambda_{K\alpha2} = 1.5444$
Step width (°); counting time (s)	0.02; 30
Angular range (°)	10–100
Pseudo-Voigt function	$PV = \eta L + (1-\eta)G$; $\eta = 0.71(2)$;
Caglioti law parameters	$U = 0.062(2)$; $V = -0.003(1)$; $W = 0.013(1)$
Number of reflections	401
Number of refined parameters	33
System; space group	Hexagonal; $R\bar{3}c$
a (Å); c (Å); V (Å^3); Z	9.1518(2); 23.1097(4); 1676.26(1); 6
R_F; R_B; R_P; R_{WP}; χ^2	0.02; 0.03; 0.08; 0.11; 1.97

powder diffraction patterns have been reported for $MTi_2(AsO_4)_3$ (M = Li, Na, Ag, K), $M_{0.5}Ti_2(AsO_4)_3$ (M = Mg, Ca, Sr) [13] and $MeZr_2(As_{1-x}P_xO_4)_3$ (Me = Na, K) [14]. The structures of $KZr_2(AsO_4)_3$ [15] and $Na_3Sc_2(AsO_4)_3$ [16] have been determined from single crystal X-ray diffraction data. Structural [17,18], electrochemical [19] and vibrational [20,21] studies of $A_3M_2(AsO_4)_3$ (A = Li, Na; M = Al, Fe, In) have been reported. Recently we initiated a program on arsenate compounds in order to compare their properties to those of the phosphates. The present paper reports on the crystal structure and vibrational spectra of $NaZr_2(AsO_4)_3$.

2. Experimental

$NaZr_2(AsO_4)_3$ arsenate powder was prepared from Na_2CO_3 dissolved in dilute nitric acid solution (I) and aqueous solutions of $ZrOCl_2{\cdot}8H_2O$ (II) and $(NH_4)H_2AsO_4$ (III) in stoichiometric proportions. After addition of (III) in (I + II) mixture at room temperature and slow evaporation at about 60 °C, the resulting powder was heated progressively at different temperatures, between 200 and 800 °C, with intermitting regrinding. The powder of $NaZr_2(AsO_4)_3$ is white.

Powder X-ray diffraction data were collected at room temperature on a Philips PW 3040 (θ−θ) diffractometer (40 kV, 40 mA). The structure of $NaZr_2(AsO_4)_3$ was refined with the Rietveld method using the program Fullprof [22]. The experimental conditions are given in Table 1.

Raman spectra were recorded using a Dilor XY Raman microprobe. The crystalline samples were excited with the 514.5 nm line of an Argon ion laser (Coherent model Innova 300). The spectral resolution was 3 cm^{-1}, the laser output power was 110 mW and the integration time 60 s. Infrared spectra were recorded on a Bruker IFS 113 v FTIR spectrometer as KBr pellets.

3. Results and discussion

3.1. Structural determination

X-ray powder diffraction pattern of $NaZr_2(AsO_4)_3$ is similar to that of $NaZr_2(PO_4)_3$ with a shift of the peaks toward lower values of 2θ Bragg's angles (Fig. 1). It was indexed assuming a hexagonal cell: $a_h = 9.1518(2)$ Å and $c_h = 23.1097(4)$ Å. All of the observed reflections are compatible with the $R\bar{3}c$

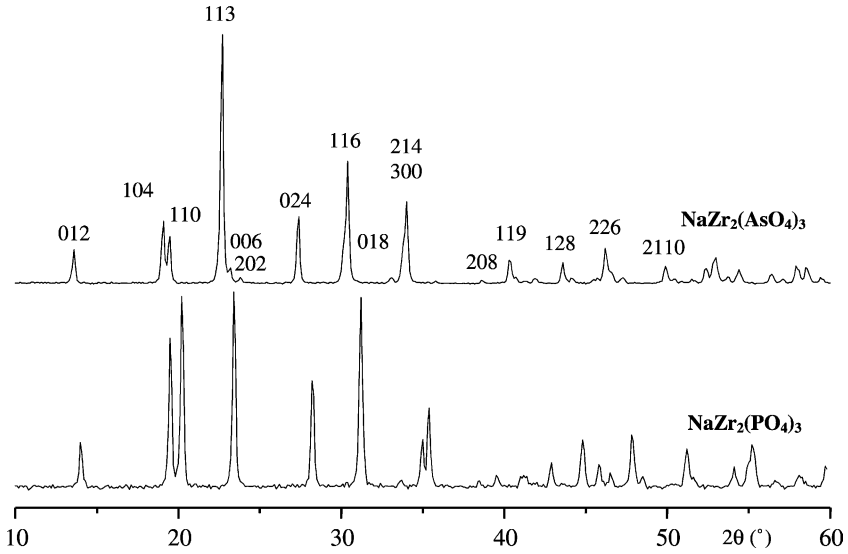

Fig. 1. X-ray powder patterns of $NaZr_2(AsO_4)_3$ and $NaZr_2(PO_4)_3$.

space group. The initial atomic coordinates used for the refinement of the structure of $NaZr_2(AsO_4)_3$ were those of the isostructural compound $NaZr_2(PO_4)_3$. After the refinement of 33 parameters (fractional atomic coordinates, temperature factors, scale factor, zero point, unit cell parameters, six background terms, profile parameters), the conventional reliability factors were: $R_p = 0.08$, $R_{wp} = 0.11$, $R_F = 0.02$ and $R_B = 0.03$. The results of the refinement as well as different structural parameters are given in Tables 1 and 2. Fig. 2 shows good agreement between the observed and calculated patterns.

The structure of $NaZr_2(AsO_4)_3$ (Fig. 3) is similar to that of $NaZr_2(PO_4)_3$ [1]. The Zr–O (2.08 Å) and As–O (1.67 Å) distances of the covalent anionic framework $[Zr_2(AsO_4)_3]$ are slightly smaller than those calculated from the ionic radii (Zr–O: 2.12 Å, As–O: 1.73 Å) [23]. Consequently the Na–O bond length

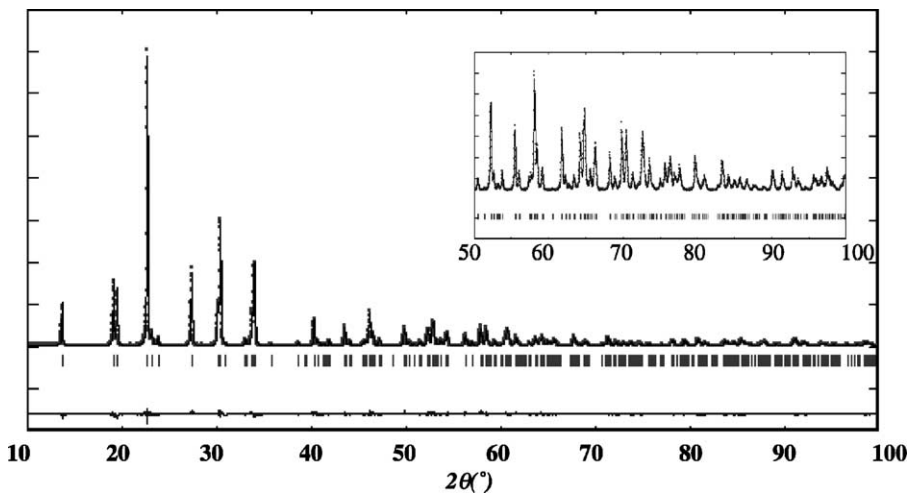

Fig. 2. Final observed (...), calculated (—) and difference X-ray profiles for $NaZr_2(AsO_4)_3$.

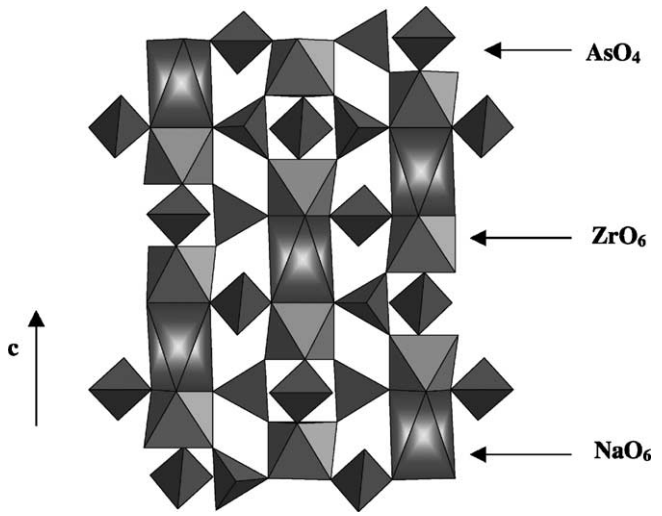

Fig. 3. Structure of $NaZr_2(AsO_4)_3$.

(2.50 Å) is larger than that obtained from the ionic radii sum of Na^+ and O^{2-} (2.42 Å) reflecting a higher degree of ionicity. Valence bond sums, $\sigma_i = \sum \exp[(R_{ij} - d_{ij})/b]$ with $b = 0.37$ Å [24], based on bond-strength analysis (Na: 0.90; Zr: 4.054; As: 5.24; O_1: 2.07; O_2: 2.05), are in good agreement with the expected formal oxidation state of Na^+, Zr^{4+}, As^{5+} and O^{2-} ions.

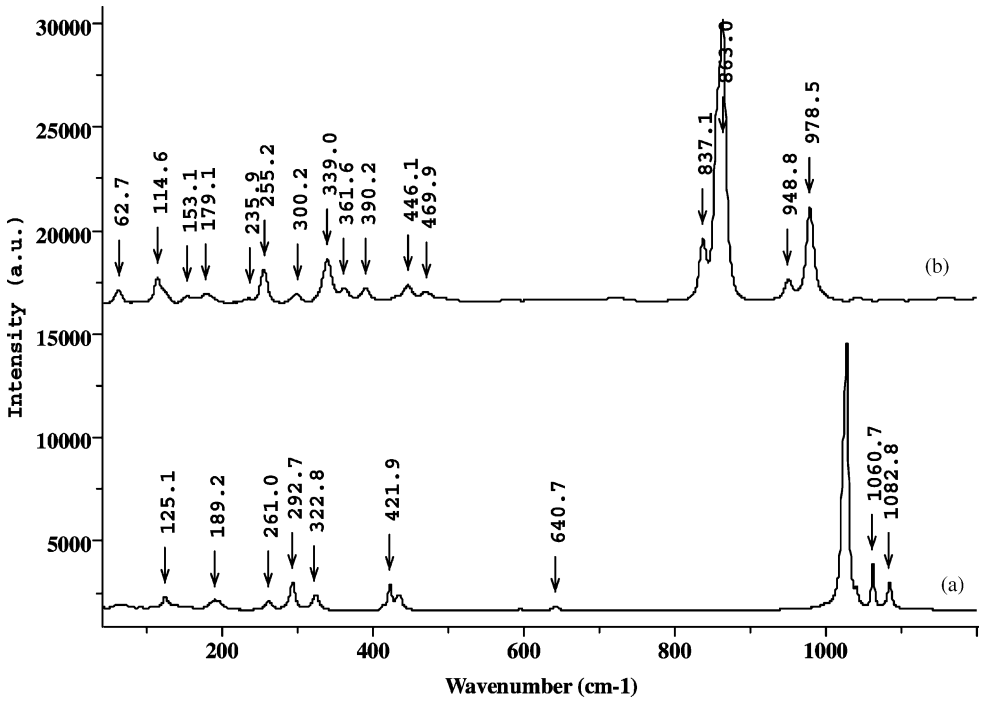

Fig. 4. Raman spectra of $NaZr_2(PO_4)_3$ (a) and $NaZr_2(AsO_4)_3$ (b).

Table 2
Atomic coordinates and isotropic temperatures factors

Atom	Wyckof site	x	y	z	$B_{iso.}$ (Å^2)	Occ.
Na	6b	0.00	0.00	0.00	3.73	1
Zr	12c	0.00	0.00	0.1436	0.09	1
As	18e	0.2903	0.00	0.2500	0.42	1
O(1)	36f	0.1811	−0.0171	0.1902	0.35	1
O(2)	36f	0.1855	0.1611	0.0833	0.45	1

Table 3 compares the cell parameters of $NaZr_2(AsO_4)_3$, $NaZr_2(PO_4)_3$ [1] and $KZr_2(AsO_4)_3$ [15]. The observed variations can be explained in the context of the Nasicon-type structure which can be considered as built of ($O_3ZrO_3M1O_3ZrO_3$) units connected by XO_4 tetrahedra (X = As, P) in three dimensions. When X is As, the lengths of the O–O tetrahedron edges increase, consequently the cell parameters of $NaZr_2(AsO_4)_3$ are superior to those of $NaZr_2(PO_4)_3$. For $AZr_2(AsO_4)_3$ (A = Na, K), the increase of c_h when sodium is replaced by potassium in M1 sites, located in the ribbons along this axis, is due to the size of K^+ ($r = 1.16$ Å) which is larger than that of Na^+ ($r = 1.00$ Å). The decrease of a_h is due to the elasticity of the network formed by polyhedra linked together only by corners. Therefore, an elongation in one direction (c_h) induces compression in the perpendicular direction (a_h).

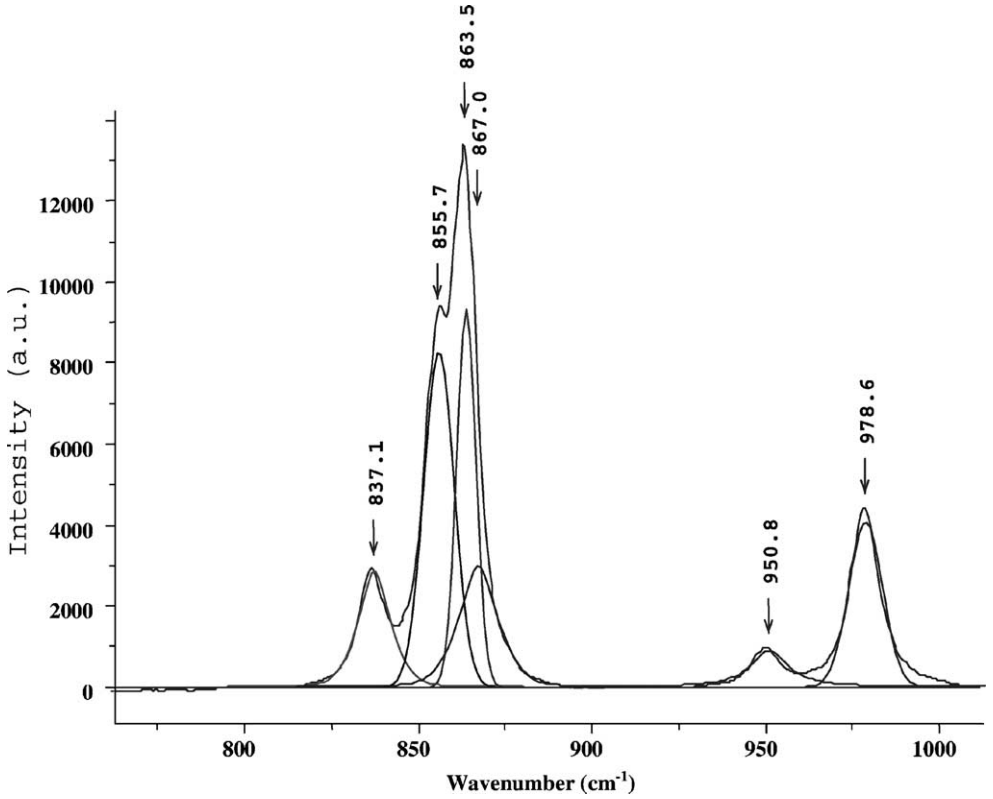

Fig. 5. Deconvoluted Raman spectrum of $NaZr_2(AsO_4)_3$ in the range of 750–1000 cm^{-1}.

Table 3
Lattice parameters of $NaZr_2(PO_4)_3$, $NaZr_2(AsO_4)_3$ and $KZr_2(AsO_4)_3$

$MZr_2(XO_4)_3$	$r(X^{5+})$ (Å)	$R(M^{+})$ (Å)	a_h (Å)	c_h (Å)	V (Å^3)
$NaZr_2(PO_4)_3$ [1]	0.170	1.02	8.80	22.75	1526
$NaZr_2(AsO_4)_3$	0.335	1.02	9.15	23.11	1677
$KZr_2(AsO_4)_3$ [15]	0.335	1.38	9.03	24.40	1722

3.2. Vibrational spectroscopy

Vibrational analysis for an isolated AsO_4^{3-} anion with point group Td leads to four modes: $A_1[(\nu_1{:}\nu_s(AsO_4)]$, $E[(\nu_2{:}\delta_s(AsO_4)]$, $2F_2[\nu_3{:}\nu_{as}(AsO_4)]$ and $[\nu_4{:}\ \delta_{as}(AsO_4)]$. All of them are Raman active whereas only ν_3 and ν_4 are infrared active. In $NaZr_2(AsO_4)_3$ ($R\bar{3}c$ space group) the arsenic site has a C_2 symmetry; therefore, we expect six Raman-active modes for the stretching vibrations; $2\nu_1(A_{1g}, E_g) + 4\nu_3$ (A_{1g}, E_g) and six IR-active modes; $\nu_1(E_u) + 5\nu_3(A_{2u}, E_u)$. For the bending vibrations we achieved eight Raman-active modes; $4\nu_2(A_{1g}, E_g) + 4\nu_4(A_{1g}, E_g)$ and seven IR-active modes; $2\nu_2(E_u) + 5\nu_4(A_{2u}, E_u)$. The external modes consist of the translational vibrations of the Na^+, Zr^{4+} and AsO_4^{3-} ions.

Fig. 4 compares Raman spectra of $NaZr_2(PO_4)_3$ and $NaZr_2(AsO_4)_3$. The shift of the peaks, toward the lower energy in the arsenate, is due to longer As–O bonds compared to P–O bonds. The high frequency part (800–1050 cm^{-1}) of the Raman spectrum of $NaZr_2(AsO_4)_3$ (Fig. 5) corresponds to the stretching vibrations of the AsO_4 tetrahedra and exhibits six peaks at 979, 951, 867, 863, 856 and 837 cm^{-1}, in good agreement with results of the factor group analysis. For the infrared spectrum (Fig. 6), four peaks (1017, 953, 870 and 855 cm^{-1}) and a shoulder (906 cm^{-1}) are observed in this region. The six Raman peaks

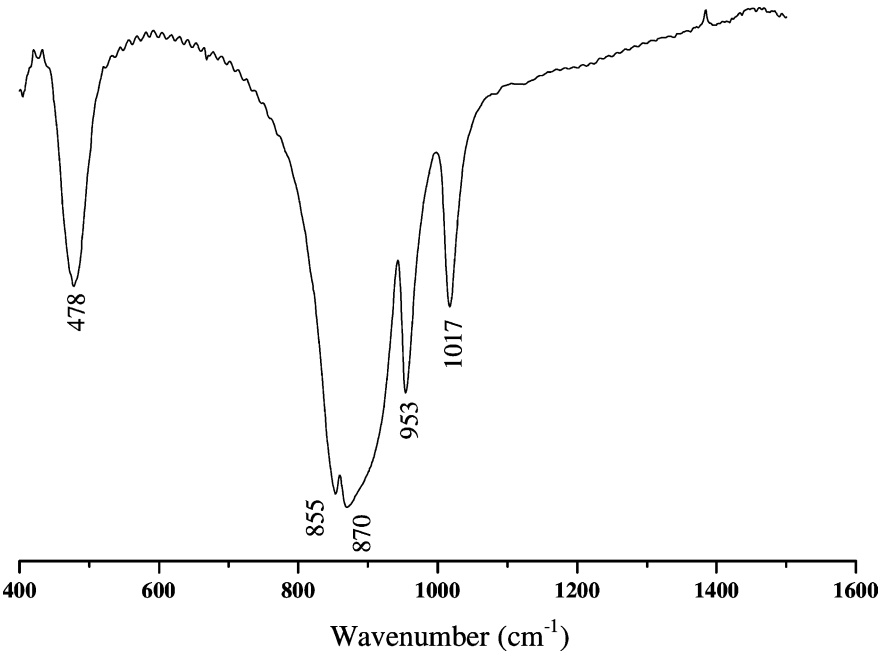

Fig. 6. Infrared spectrum of $NaZr_2(AsO_4)_3$.

observed at 470, 446, 390, 362, 339 and 300 cm^{-1} are assigned to the As–O bending vibrations, the predicted ones are eight. The peaks situated below 300 cm^{-1} are attributed to the external modes; seven Raman peaks (255, 236, 179, 153, 124, 115 and 63 cm^{-1}) are observed between 250 and 50 cm^{-1}.

4. Conclusion

The arsenate $NaZr_2(AsO_4)_3$ has been synthesised and characterized by mean of X-ray diffraction and vibrational spectroscopy. Its structure has been solved in $R\bar{3}c$ space group. It is formed by a 3D network of ZrO_6 octahedra and AsO_4 tetrahedra linked by corners. The sodium is at the centre of the antiprism located between tow ZrO_6 octahedra. Assignments of internal modes of the AsO_4 tetrahedra have been made. The number of the peaks observed, in Raman and infrared spectra, is in good agreement with that predicted by the factor group analysis of the $R\bar{3}c$ space group.

Acknowledgements

The authors would like to thank Dr. J.P. Chaminade (ICMCB-CNRS, France) and Professor A. Lachgar (Wake Forest University, USA) for their useful support.

References

[1] L.O. Hagman, P. Kierkegaard, Acta Chem. Scan. 22 (1968) 1822.
[2] H.Y.-P. Hong, Mater. Res. Bull. 11 (1976) 173.
[3] J.B. Goodenough, H.Y.P. Hong, J.A. Kafalas, Mater. Res. Bull. 11 (1976) 203.
[4] F. Cherkaoui, J.C. Viala, C. Delmas, P. Hagenmuller, Solid State Ionics 21 (1986) 333.
[5] C. Delmas, A. Nadiri, J.L. Soubeyroux, Solid State Ionics 28-30 (1988) 419.
[6] J.L. Rodrigo, P. Carrasco, J. Alamo, Mater. Res. Bull. 24 (1989) 611.
[7] I. Bussereau, R. Olazcuaga, J.M. Dance, C. Delmas, G. Le Flem, A. El Jazouli, J. Alloys and Compounds 188 (1992) 120.
[8] B.L. Cushing, J.B. Goodenough, J. Solid State Chem. 162 (2001) 176.
[9] A. Aatiq, C. Delmas, A. El Jazouli, J. Solid State Chem. 158 (2001) 169.
[10] R. Masse, A. Durif, J.C. Guitel, I. Tordjmman, Bull. Soc. Mineral. Crystallogr. 95 (1972) 45.
[11] S. Krimi, A. El Jazouli, A. Lachgar, L. Rabardel, D. de Waal, J. R. Ramos–Barrado, Ann. Chim. Sc. Mat. 25 (Suppl.) (2000) S75.
[12] S. Krimi, I. Mansouri, A. El Jazouli, J.P. Chaminade, P. Gravereau, G. Le Flem, J. Solid State Chem. 105 (1993) 561.
[13] A. Yaakoubi, T. Jouini, N. Jouini, C. R. Acad. Sci. Paris T312 (1991) 451.
[14] D. Mazza, M. Lucco-Borlea, S. Ronchetti, Powder Diff. 13 (1998) 227.
[15] M. El Brahimi, J. Durand, Z. Anorg. Allg. Chem 584 (1990) 178.
[16] W.T.A. Harrison, M.L.F. Phillips, Acta Cryst. C57 (2001) 2.
[17] C. Masquelier, F. d'Yvoire, G. Collin, J. Solid State Chem. 118 (1995) 33.
[18] K. H Lii, J. Ye, J. Solid State Chem. 131 (1997) 131.
[19] C. Masquelier, A.K. Padhi, K.S. Nanjundaswamy, J.B. Goodenough, J. Solid State Chem. 135 (1998) 228.
[20] S. Khorari, A. Rulmont, P. Tarte, J. Solid State Chem. 134 (1997) 31.
[21] J.M. Winand, A. Rulmont, P. Tarte, J. Solid State Chem. 87 (1990) 83.
[22] J. Rodriguez Carvajal, Collected Abstract of Powder Diffraction Meeting, vol. 127. Toulouse, France, 1990.
[23] R.D. Shannon, Acta Cryst. A32 (1976) 751.
[24] I.D. Brown, D. Altermatt, Acta Cryst. B41 (1985) 244.